Large-eddy simulation of supersonic reacting flows

By G. Ribert, L. Bouheraoua AND P. Domingo

CORIA - UMR6614 CNRS, INSA and Université de Rouen, Normandie Université
Avenue de l'Université, 76800 St-Etienne-du-Rouvray, France

Large eddy simulations of a supersonic hydrogen-air burner have been performed with the SiTComB numerical code. A reduced kinetic scheme is used and chemical source terms are evaluated based on resolved quantities. Three mesh resolutions have been considered: 2, 30 and 113 million of points (MP). With 2MP the flame is unstable and no comparison with experimental data becomes possible. However, the flame lift-off height is over predicted for the case 30MP. Refining the mesh (113MP) improves the capture of mixing and the flame lift-off height gets close to the experimental results. However this case must be be further converged to get accurate and final conclusions. Scatterplots of temperature and species mass fractions follows the trends already observed in past studies.
A lookup table of auto-ignition is built for different levels of pressure and composition corresponding to the values found in the large-eddy simulation. Delays of auto-ignition are found of the order of magnitude of the time required to convect a pocket of pure fuel at a constant speed equal to the fuel inlet velocity.

1. Introduction

Supersonic combustion has obtained an increasing interest these last decades for the development of hypersonic air-breathing propulsion systems such as scramjets engines. However, a number of issues have still to be clarified as this technology is not viable yet. Indeed the flame stabilization in an high speed environment is a technological issue: fuel-air mixing and flame-holding can be inefficient due to slow kinetic rates and very short combustor residence time [1,2]. An analysis of the combustion processes in a supersonic environment must then be carefully performed. To overcome these issues, cavities have been introduced into the architecture of combustion chambers [3, 4] to create a low-speed zone where mixing and combustion can efficiently take place. Cavity shape and injectors location are of particular interest as they impact the flame position and blowout limits [5]. For example near rich blowout, floor injectors provide advantages because unburned fuel can escape through the shear layer. Although some flight tests have successfully demonstrated the feasibility of scramjet engines such as in the last X-51A flight [6], experimental studies dealing with supersonic combustion are scarce because they require a large investment and present numerous difficulties. Numerical simulations have then appeared to be a good alternative for the study of configurations involving supersonic non-reactive and reactive flows. Despite the increase in high-performance technical computing, ensuring the accuracy of the methods and models used in numerical simulation remains a difficult task.

As supersonic engines often involve solid devices placed in the supersonic flow, a model such as Immersed Boundary Methods (IBMs) to describe complex geometries is required in the numerical methodology. The main advantage of this concept is the relative simplicity of the governing equations in Cartesian coordinates, and the simple grid generation. First introduced by Peskin [7], these methods which use a formulation of forcing terms on desired surfaces, were mostly applied to a wide range of incompressible flow configurations. However, application to fully compressible flows configurations are scarce [8, 9].

In this paper, we report LES of the supersonic turbulent burner of Cheng and Wehrmeyer [10] where a hydrogen injection flows at Mach 1, surrounded by hot gases flowing at Mach 2. Accurate data for dynamics, mixing and combustion modes are available. This co-flowing hydrogen-air burner produces an axisymmetric flame which comports a large induction mixing zone due to massive convection, and above which the lifted flame stabilizes. The main flame stabilization position has been measured at 25 diameters from the burner exit. The numerical strategy focusses on the effect of the shear layer prediction on the flame stabilization position. The reduced mechanism used in this study involves three steps and five reactive species. It was validated for a wide range of premixed and non-premixed laminar flames from previous studies [11, 12]. Finally, tabulated chemistry of auto-ignition is investigated for an a priori analysis of the flow field.

2. Simulation setting-up

2.1. *Numerics*

The supersonic burner (SSB) of Cheng *et al.* [10] is investigated with SiTComB (Simulation of Turbulent Combustion with Billion of points) numerical code [16–20], which solves the unsteady compressible reacting Navier-Stokes equation system on Cartesian meshes. It was mainly designed to perform Direct Numerical Simulation (DNS) and highly resolved Large Eddy Simulation (LES) on thousands of processors. The numerical method consists of integrating the balance equations of momentum, total energy and species mass fractions with a fourth-order skew-symmetric scheme, augmented with second and fourth-order artificial terms [21] in order to suppress spurious oscillations. A fourth-stage Runge-Kutta scheme is used for time advancement. The inlet/outlet boundaries are described using the three-dimensional Navier-Stokes characteristic boundary conditions approach [22] thus ensuring numerical stability and minimal acoustic reflections.

2.2. *Chemistry*

The chemistry used to simulate the Cheng's burner has been developed by Boivin et al. [11]. It is a reduced kinetic scheme that comes from the mechanism of San Diego [13]. This detailed mechanism has 21 reversible elementary involving 8 reacting species (H_2, O_2, H_2O, H, O, OH, HO_2, H_2O_2). A steady state for species O, OH, and H_2O_2 is assumed. The resulting three-step mechanism is:

$$3H_2 + O_2 \rightleftharpoons 2H_2O + 2H$$
$$H + H + M \rightleftharpoons H_2 + M$$
$$H_2 + O_2 \rightleftharpoons HO_2 + H$$

These three chemical reaction rates, with their correction terms [11] have then been implemented into SiTComB, and validated on the simulations of stirred reactors. A good

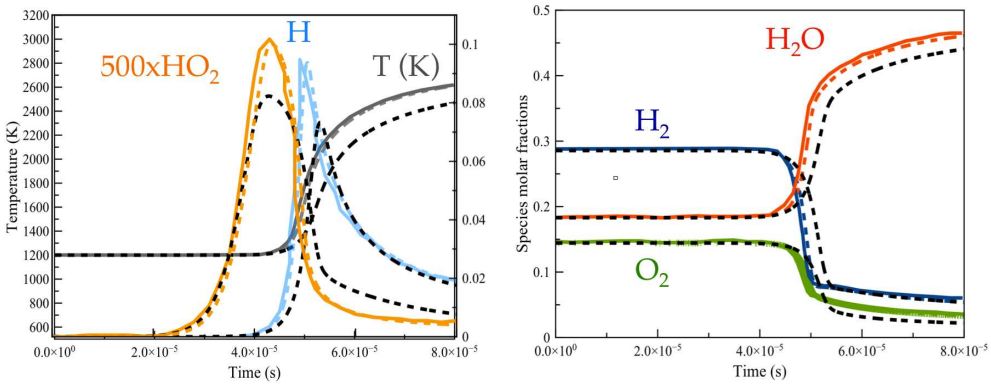

(a) (b)

FIGURE 1. Auto-ignition simulation: pressure is set to 1 atm and inlet temperature is 1200 K. Dash lines are present computations and solid lines are from Boivin et al. [11]. Color lines are for reduced chemistry and black lines are detailed chemistry.

agreement has been found with the validations provided by Boivin et al. [11] as shown in [15] on the delay of auto-ignition. In addition, similar simulations have been performed with Senkin package [14] in order to compare the temporal profiles of species provided by Boivin's both reduced and detailed chemistry. Here again a good agreement is observed in Figs. 1 when using the reduced chemistry. However, using the detailed chemistry leads to a longer auto-ignition delay and a smaller magnitude for intermediate species such as H or HO_2. Cheng's burner simulation will be performed using Boivin's reduced chemistry without any subgrid scale modeling for the chemical source term $(\dot{\omega}_k)$ of the k transported species. This means that the filtered species chemical source terms are based on resolved values: $\widetilde{\dot{\omega}_k} = \dot{\omega}_k(\tilde{p}, \tilde{T}, \tilde{Y}_k)$. This latter relation may be a strong approximation which will have to be addressed in future work.

2.3. *Supersonic burner*

The experiment sketched in Fig. 2(a) consists of a pure hydrogen jet injected at sonic speed into a supersonic (Mach 2) co-flow of hot products generated by a lean combustor. The hydrogen is burned with the air-enriched oxygen, and the vitiated air is accelerated through a convergent-divergent nozzle. The exit conditions are given in Table 1. Experimental data for temperature and species are available at distances $x/D = 0.85, 10.8, 21.5, 32.3, 43.1, 64.7$ and 86.1 from the burner exit (Fig. 2(b)), with D being the fuel injector inner diameter. Computations have been performed with a Cartesian mesh about 30 millions of points (case 30M), with a very refined mesh near the burner area: the cell size is $0.14 < \Delta x < 0.45$ mm for $x/D < 40$. This mesh refinement follows the recommendation of Boivin et al. [12], thus ensuring a resolution well enough to solve mixing and ignition without the need of a turbulent combustion model in this area. No explicit sub-grid scale modeling is used for the turbulent viscosity term. The inlet velocity, temperature and species mole fractions have been approximated to match with the nominal experimental exit conditions of Table 1. In addition, a 20% homogeneous isotropic turbulence has been injected in the co-flow, as mentioned in the experiment [10]. A second mesh discretization has been used where the cell size is divided by 1.75 in the region of interest leading to a total mesh points about 113 million (case 113M). Finally, several simulations on a coarse mesh of 2 million of points has been performed with different

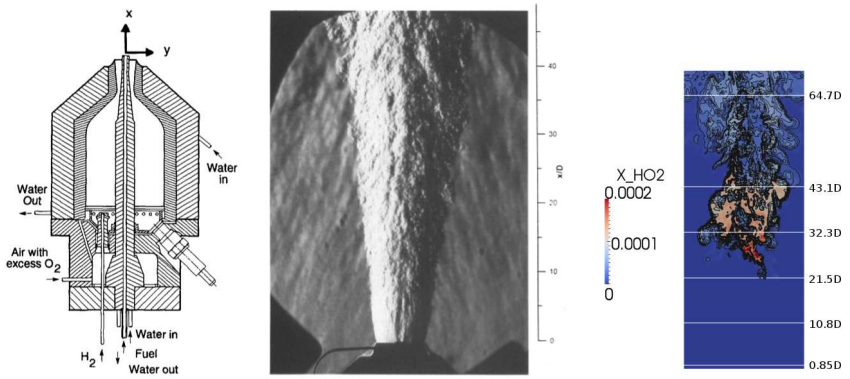

(a) (b) (c)

FIGURE 2. Sketch of Cheng's supersonic burner injection system (a), schlieren photography of the jet (b) and numerical instantaneous HO_2 mole fraction in the center plane of the flame (case 30M) with contour lines plotted every 2.10^{-5} (c).

Parameter	
Air mass flow rate (±2%)	0.0735 kg/s
H_2 mass flow rate (±2%)	0.000173 kg/s
O_2 mass flow rate (±3%)	0.0211 kg/s
fuel mass flow rate (±3%)	0.000362 kg/s
Nozzle exit inner diameter	17.78 mm
Fuel injector inner diameter	2.36 mm
Fuel injector outer diameter	3.81 mm
Vitiated air exit conditions	
Pressure	107 kPa
Temperature	1250 K
Mach Number	2.0
Velocity	1420 m/s
O_2 mole fraction	0.201
N_2 mole fraction	0.544
H_2O mole fraction	0.255
Fuel exit conditions	
Pressure	112 kPa
Temperature	540 K
Mach Number	1.0
Velocity	1780 m/s
H_2 mole fraction	1.0

TABLE 1. Operating conditions of the SSB burner.

mesh arrangements during this Summer Program without success to get a stabilized flame.

Note that it was shown [10, 11] that the mixing and ignition processes are mostly controlled by the dynamics of the shear layer produced downstream of the hydrogen injector

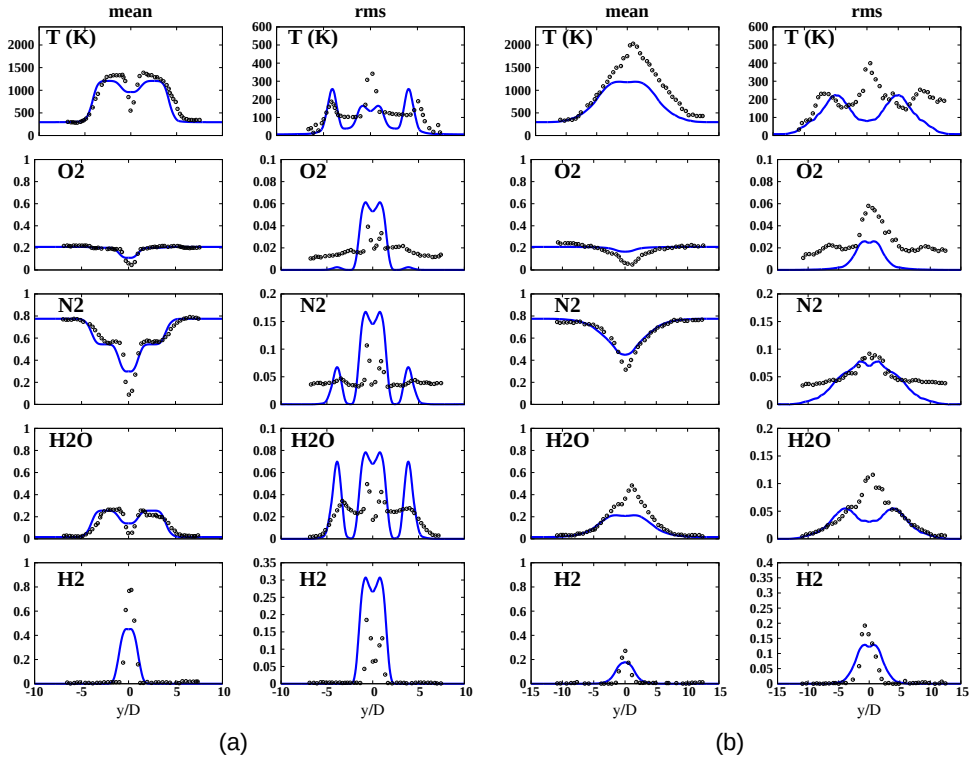

FIGURE 3. Mean and rms temperature and molar fraction profiles at (a) $x/D = 10.8$ and (b) $x/D = 32.3$. Measurements are represented by circles and solid lines correspond to case 30M without IBM.

lips, thus enhancing the fuel-air mixing. As a consequence, starting the computational domain at the burner exit ($x/D = 0$), or inside the hydrogen injector lips ($x/D = -1.55$), shows a slightly different flow field and shock patterns [15].

3. Results and discussion

As experimentally observed by Cheng et al. [10], a lifted flame appears controlled by the mixing of the cold hydrogen stream with the hot vitiated air. In Fig. 2(c), an instantaneous snapshot of the HO_2 mole fraction is shown for the case 30M and a good agreement is found with previous numerical studies [12]. The lift-off height ranges from $x/D = 20$ to $x/D = 30$, which is reasonable compared to the experimental value of $x/D = 25$. The three-step reduced scheme seems good enough to predict autoignition processes in H_2/air combustion [11]. Fig. 3 reports experimental and numerical radial profiles for mean values and rms fluctuations of the temperature and species mole fractions, at two downstream locations $x/D = 10.8$ and 32.3. Since no measurements were reported at the burner exit, most previous numerical studies use the experimental data at $x/D = 0.85$ as inlet profiles [12]. In the present study, an excellent agreement has been found at $x/D = 0.85$ validating the aerodynamic injected profiles. Results at positions $x/D = 10.8$ and $x/D = 32.3$ correspond to the induction zone and to the flame brush, respectively. In Fig. 3(a), the influence of the shear layers coming from the injector lips are

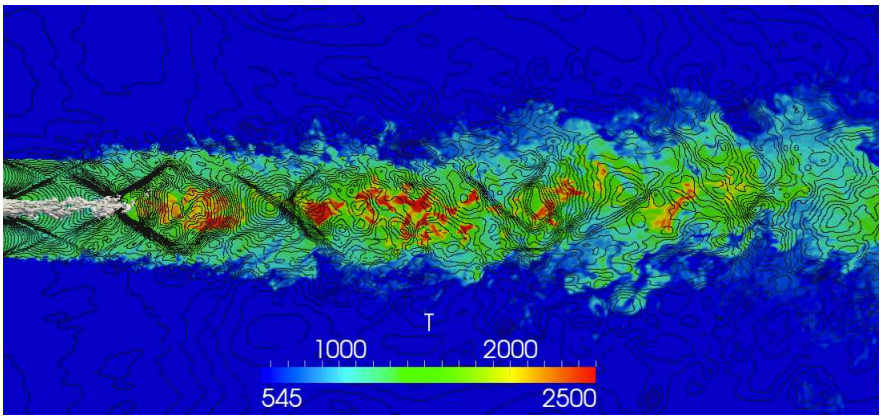

FIGURE 4. Field of temperature (case 113M) with shock patterns (black) and hydrogen jet (white).

clearly visible (two peaks) on the mean temperature and H_2O mole fraction profiles when close to the burner. These peaks will vanish around $x/D = 21.5$ meaning a complete fuel air mixing occurred. However, the mean profiles have non negligible errors in magnitude, particularly for the temperature and the H_2 mole fraction. These under-predictions are due to the fact that autoignition occurs later compared to the experiment, and leads to an under-prediction of temperatures. Magnitude of rms fluctuations are mainly coherent with measurements, with a over-prediction in the mixing zone and an under-prediction in the flame zone.

Refining the mesh (case 113M) improves the flow field description. Auto-ignition process appears earlier than in case 30M. As a consequence it is expected a better description of the temperature profile at $x/D = 32.3$ but simulations must still be converged. A diamond-shock structure, relative to the higher oxidizer injection pressure, is observed along the entire domain. The pressure range is 1.6 bar meaning that the reaction zones may experience different pressure levels. Based on case 113M, a scatterplot of temperature, H_2O, O_2, H_2 and N_2 mass fractions as a function of the mixture fraction, f, is shown for locations $x/D = 10.8$ (Fig. 5) and $x/D = 25.0$ (Fig. 6), position of the mean experimental flame lift-off height. The mixture fraction f is defined as

$$f = \frac{Z_H - Z_{H,coflow}}{Z_{H,fuel} - Z_{H,coflow}}, \tag{3.1}$$

with, Z_H the hydrogen elemental mass fraction in the mixture given by $Z_H = \sum \mu_{i,H} Y_i$ where $\mu_{i,H}$ denotes the mass proportion of atomic hydrogen in the species i, and Y_i are their mass fractions. Close to the injector exit (Fig. 5), scatterplots are clearly located on mixing lines either for the experimental data, Boivin's simulation or the present results. Moving downstream leads to more dispersed results ranging from mixing to equilibrium lines meaning that the combustion is not complete yet (Fig. 6). In Fig. 7, the scatterplot of the energy source term $(\dot{\omega}_T)$ is plotted as a function of pressure for two locations, x/D = 10.8 and 25.0. At x/D = 10.8 (Fig. 7(a)), we are located just behind the first diamond shock pattern, where the flame starts to ignite. The pressure is quasi-constant around 150 kPa. Downstream in the flame (Fig. 7(b)), $\dot{\omega}_T$ is spread over a range of pressure from 70 kPa to 200 kPa with a maximum still located at 150 kPa. In Fig. 8, the field of source term of energy is shown with shock patterns. Some low levels of $\dot{\omega}_T$ may

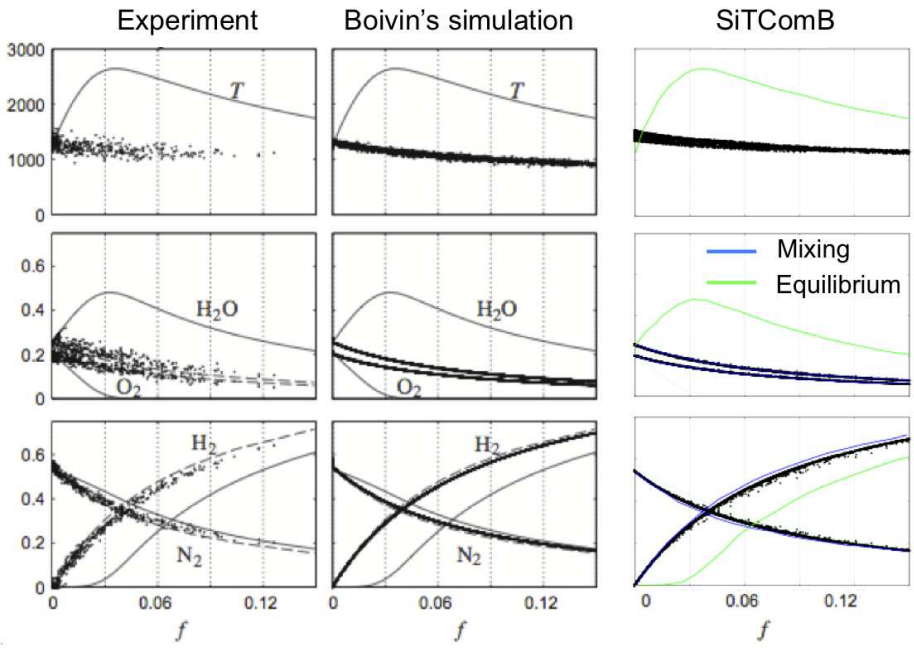

FIGURE 5. Scatterplots at $x/D = 10.8$.

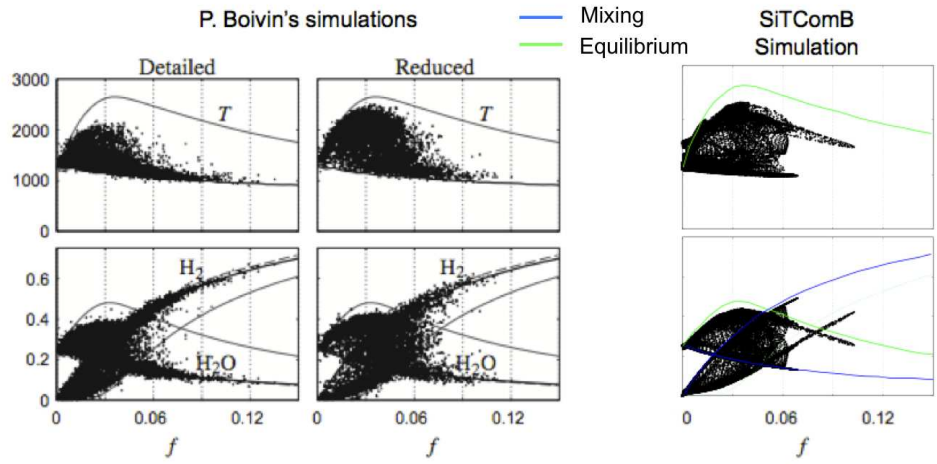

FIGURE 6. Scatterplots at $x/D = 25.0$.

be observed inside the first diamond shape, but clear auto-ignition starts only inside the second diamond shape. Then, the flame starts to develop, however simulation must still be converged for comparisons with available experimental data.

4. Conclusions and perspectives

The supersonic combustion encountered in the Cheng's burner has been studied with large-eddy simulations and a reduced chemistry. Three levels of mesh refinement were

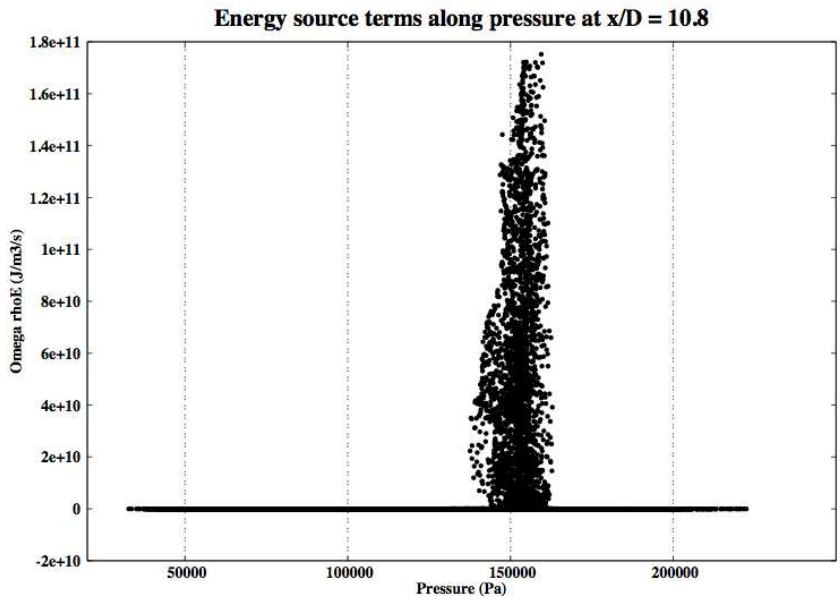

(a) Location $x/D = 10.8$

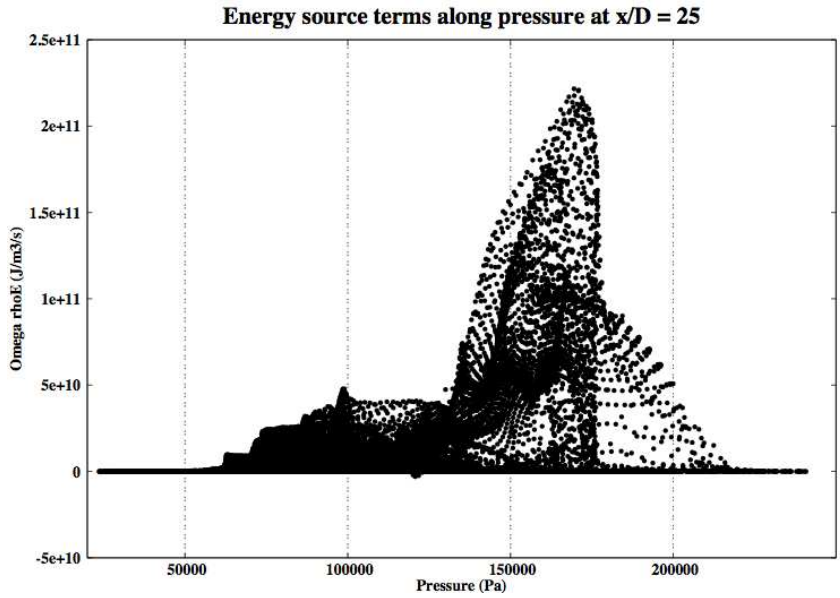

(b) Location $x/D = 25.0$

FIGURE 7. Scatterplots of energy source term as a function of pressure.

used. For the very coarse mesh, the flame is unstable. For the intermediate mesh, the simulation follows the trend already observed in past studies, but improvements must be realized to match with the experimental data in the flame brush. Best results are found when the mixture between the fuel and the vitiated air is well captured, *i.e.* with a finer mesh. These results must still be converged for comparison with experimental data. However, the mesh resolution may be not high enough to handle direct numerical sim-

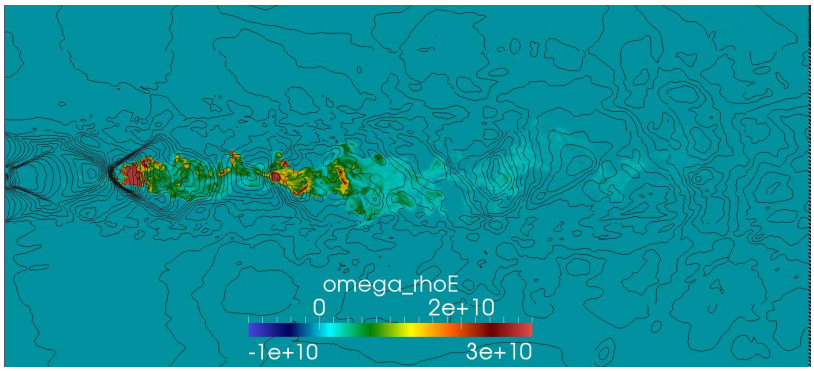

FIGURE 8. Field of the energy source term (case 113M) with shock patterns (black).

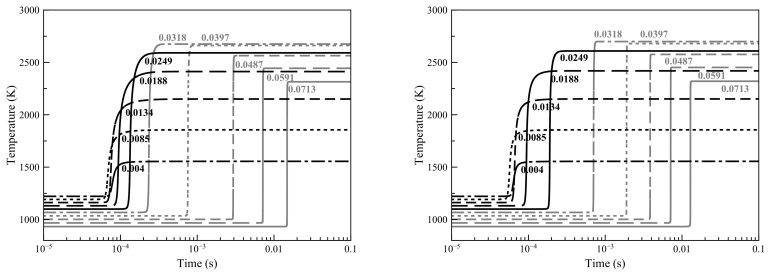

(a) Pressure: 100 kPa (b) Pressure: 150 kPa

FIGURE 9. Time evolution of the temperature for auto-ignition simulations performed with the Senkin package [14] at different levels of mixture.

ulation and the importance of adding a sub grid scale combustion modeling should be explored. Using tabulated chemistry would reduce the CPU cost and facilitate the introduction of a subgrid model. This point has been partially addressed by comparing delay of auto-ignition found in laminar simulations and the order of magnitude of the time required to fire the fresh mixture, $3.3\ 10^{-5}$ s, approximated by the flame liftoff height divided by the fuel inlet velocity. Both are similar meaning that tabulated chemistry is a path worth to explore for supersonic combustion modeling. This point is shown in Figs. 9 where the time evolution of the temperature for auto-ignition simulations is plotted for different levels of mixture ($Z = [Y_{N_2} - Y_{N_2}^{VG}]/Y_{N_2}^{VG}$) with $Y_{N_2}^{VG}$ being the mass fraction of N_2 in the vitiated gas stream. This observation can be made for the pressure values encountered in the results of the LES 113M case.

Acknowledgments

Financial support has been provided by the German Research Foundation (Deutsche Forschungsgemeinschaft – DFG) in the framework of the Sonderforschungsbereich Transregio 40. Computations were performed using HPC resources from CRIHAN and GENCI [CCRT/CINES/IDRIS] (France).

References

[1] MAAS, U. AND POPE, S. (1992). Simplifying chemical kinetics: intrinsic low-dimensional manifolds in composition space. *Combust. Flame*, **88**(3), 239–264.

[2] MAURICE, L., EDWARDS, T. AND GRIFFITHS, J. (2000). Liquid hydrocarbon fuels for hypersonic propulsion. *AIAA J.*, 757–822.

[3] DAVIS, D. AND BOWERSOX, R. (1997). Computational fluid dynamics analysis of cavity flame holders for scramjets. *AIAA Paper 97-3270*.

[4] BEN-YAKAR, A. AND HANSON, R. (2001). Cavity flame-holders for ignition and flame stabilization in scramjets: an overview. *J. Propul. Power*, **17**(4), 869–877

[5] GHODKE, C., PRANATHARTHIKARAN, J., RETAUREAU, G. AND MENON, S. (2011). Numerical and Experimental Studies of Flame Stability in a Cavity Stabilized Hydrocarbon-Fueled Scramjet. *AIAA Paper 2011-2365*.

[6] HANK, J. M., MURPHY, J. AND MUTZMAN, R. (2008). The X-51A scramjet engine flight demonstration program. *AIAA Paper 2008-2540*.

[7] PESKIN, C. S. (1977). Numerical analysis of blood flow in the heart. *J. Comput. Phys.*, **25**, 220–252.

[8] CHAUDHURI, A., HADJADJ, A. AND CHINNAYYA, A. (2011). On the use of immersed boundary methods for shock/obstacle interactions. *J. Comput. Phys.*, **230**, 1731–1748.

[9] MERLIN, C., DOMINGO, P. AND VERVISCH, L. (2013). Immersed boundaries in large eddy simulation of compressible flows. *Flow Turbul. Combust.*, **90**, 29–68.

[10] CHENG, T., WEHRMEYER, J., PITZ, R., JARRETT, O. AND NORTHAM, G. (1994). Raman measurement of mixing and finite-rate chemistry in a supersonic hydrogen-air diffusion flame. *Combust. Flame*, **99**, 157–173.

[11] BOIVIN, P., JIMENEZ, C., SANCHEZ, A. AND WILLIAMS, F. (2011). An explicit reduced mechanism for H2-air combustion. *Proc. Combust. Inst.*, **33**, 517–523.

[12] BOIVIN, P., DAUPTAIN, A., JIMENEZ, C. AND CUENOT, B.. (2012). Simulation of a supersonic hydrogen–air autoignition-stabilized flame using reduced chemistry. *Combust. Flame*, **159**(4), 1779–1790

[13] SAXENA, P. AND WILLIAMS, F. (2006). Testing a small detailed chemical-kinetic mechanism for the combustion of hydrogen and carbon monoxide. *Combust. Flame*, **145**(1-2), 316–323.

[14] LUTZ, A., KEE, R. AND MILLER, J. (1988). Senkin: a fortran program for predicting homogeneous gas phase chemical kinetics with sensitivity analysis. *SAND87-8248 Report*.

[15] BOUHERAOUA, L., RIBERT, G., DOMINGO, P. AND LARTIGUE, G. (2013). Large Eddy Simulation of supersonic non-reactive and reactive flows with an Immersed Boundary Method. *5th EUCASS Conf., Munich, Germany*.

[16] DOMINGO, P., VERVISCH, L. AND BRAY, K. (2002). Partially premixed flamelets in LES of nonpremixed turbulent combustion. *Combust. Theory Model.*, **6**(4), 529–551.

[17] DOMINGO, P., VERVISCH, L., PAYET, S. AND HAUGUEL, R. (2005). DNS of a premixed turbulent V flame and LES of a ducted flame using a FSD-PDF subgrid scale closure with FPI-tabulated chemistry. *Combust. Flame*, **143**, 566–586.

[18] DOMINGO, P., VERVISCH, L. AND VEYNANTE, D. (2008). Large-eddy simulation of a lifted methane jet flame in a vitiated coflow. *Combust. Flame*, **152**, 415–432.

[19] RIBERT, G., TAIEB, D., PETIT, X., LARTIGUE, G. AND DOMINGO, P. (2013). Simulation of supercritical flows in rocket-motor engines: application to cooling channel and injection system. *Eucass Book Series: Prog. Propuls. Physics*, **4**, 205–226.

[20] http://www.coria-cfd.fr/index.php/SiTCom-B

[21] TATSUMI, S., MARTINELLI, L. AND JAMESON, A. (1995). Flux-limited schemes for the compressible Navier-Stokes equations. *AIAA J.*, **33**(2), 252–261.

[22] LODATO, G., VERVISCH, L. AND DOMINGO, P. (2008). Three-dimensional boundary conditions for direct and large-eddy simulation of compressible viscous flows. *J. Comput. Phys.*, **227**, 5105–5143.